View metadata, citation and similar papers at core.ac.uk

brought to you by CORE

provided by University of Bath Research Portal

Citation for published version:
Mohammadi, A, Abdelkhalek, M & Sadrafshari, S 2020, 'Resonance Frequency Selective Electromagnetic Actuation for High-Resolution Vibrotactile Displays', *Sensors and Actuators A-Physical*, vol. 302, 111818. https://doi.org/10.1016/j.sna.2019.111818

DOI:
10.1016/j.sna.2019.111818

Publication date:
2020

Document Version
Peer reviewed version

Link to publication

Publisher Rights
CC BY-NC-ND

University of Bath

Alternative formats
If you require this document in an alternative format, please contact:
openaccess@bath.ac.uk

General rights
Copyright and moral rights for the publications made accessible in the public portal are retained by the authors and/or other copyright owners and it is a condition of accessing publications that users recognise and abide by the legal requirements associated with these rights.

Take down policy
If you believe that this document breaches copyright please contact us providing details, and we will remove access to the work immediately and investigate your claim.

Download date: 04. Feb. 2021

Resonance Frequency Selective Electromagnetic Actuation for High-Resolution Vibrotactile Displays

Ali Mohammadi, Mahmoud Abdelkhalek, Shamin Sadrafshari

***Abstract*— Vibrotactile displays offer significant potential for conveying information through the sense of touch in a wide variety of applications. Spatial resolution of these displays is limited by the large size of actuators. We present a new selective electromagnetic actuation technique to control the vibrations of multiple tactile elements using a single coil based on their individual mechanical resonance frequencies. This technique allows low-cost and highly reliable implementation of many tactile elements on a smaller area. A prototype is manufactured using 3D-printed tactile elements and off-the-shelf coils to characterize the proposed technique. This prototype successfully increases the resolution by 100% from 16 to 32 tactile pixels (taxels) on a 25cm^2 pad, without sacrificing other performance metrics such as refresh rates and power consumption. The multiphysics finite element analysis developed for this new actuation technique are experimentally validated by optical vibrometry measurements. This work demonstrates the capability of resonance-selective electromagnetic actuator in developing high-resolution low-cost vibrotactile displays.**

***Index Terms*— Vibrotactile display, electromagnetic actuator, spatial resolution, frequency multiplexing, resonance frequency**

I. Introduction

Vibrotactile displays have been under intense investigation as human-machine interface (HMI) devices with potential applications in virtual training for surgeons, remotely touching materials via the Internet, automotive industry, active interfaces for blind persons, and sensory substitution devices [1]. These devices have been implemented using arrays of transducers to convey graphical information through the sense of touch. Different transduction mechanisms such as electro-tactile [2], piezoelectric [3, 4] and electromagnetic [5-7] have been approached to convert the electrical signals, generated by pixelated graphical information in computers or mobile phones, to tactile stimulus. However, each of these transduction mechanisms suffer from certain deficiencies that hinder real-world application of tactile displays. Spatial resolution is among the most stringent constraints, which severely limit the information conveyed by these HMI devices. This problem has been approached in different ways. For example, high resolution electro-tactile transducers presented in [2] are limited by the stimulation depth especially with Pacinian corpuscles and an "electrical" sensation. Piezoelectric actuators within these dimensions have limited travel ranges. The high resolution piezoelectric device introduced in [3] can only generate lateral vibrations. Another piezoelectric scissor-shaped microactuator presented in [4] increases the travel range while the area occupied by each tactile element (around 30mm^2) limits the resolution. Several contributions have been made to increase the resolution of electromagnetic actuators. The recent electromagnetic tactile display presented in [5] feature 4mm pin-shaped taxels with 8mm pitches. In order to achieve higher resolution some researchers investigate the solutions offered in microelectromechanical systems (MEMS) [8], which are limited by intrinsic MEMS deficiencies. The high-resolution electro-vibration technique presented in [9] is extremely fragile. A coil array that excite permanent magnets attached to flexible diaphragm is presented in [6]. However, integration of permanent magnets and/or high quality coils in MEMS is still a microfabrication challenge [10].

The resolution bottleneck is mainly related to the physics of actuators. Each tactile element in all existing vibrotactile displays is actuated by one individual actuator. These actuators can only transform limited amount of electrical to mechanical energy in certain dimensions. For example, the mechanical force generated by a coil in response to supplied electrical current is limited by the coil dimensions, that can tolerate certain amount of electrical power. Figure 1 illustrates our preceding 4×4 tactile array prototype, wherein ferromagnetic

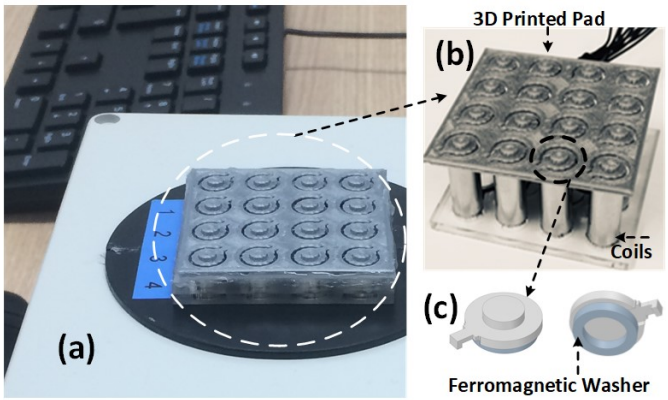

Fig. 1. A 4×4 electromagnetic vibrotactile display interfaced to personal computer, a) the vibrotactile display with microcontroller and interface electronics enclosed, (b) the array of off-the-shelf coils underneath the 3D printed taxels pad, (c) The taxel 3D model, top view (left) and bottom view (right).

Dr Ali Mohammadi (corresponding author) and Dr Shamin Sadrafshari are with the Department of Electronic and Electrical Engineering, University of Bath, UK.
Mr Mahmoud Abdelkhalek is pursuing a Master's degree at the Department of Electrical and Computer Engineering, North Carolina State University, US.

parts (stainless steel washers) are glued underneath the 3D printed Poly-Lactic Acid (PLA) taxel array to respond to the electromagnetic field generated by coils. As an alternative we also developed taxels in PLA material with impregnated ferromagnetic powder for 3D printing, which was not as responsive as the stainless steel washers glued to the plastic printed taxels. The 3D model of these taxels are illustrated in Figure 1c. The 25 cm^2 taxel pad is fixed on a corresponding coil matrix array developed by off-the-shelf solenoid coils as shown in Figure 1b. A microcontroller and power amplifier interface circuit are used to map computer generated 4×4 matrices to this array to through the serial port.

Building up on this prototype, we present a new actuation technique to vibrate multiple taxels individually using a single solenoid coil actuator. This new approach offers a robust and low-cost solution to mitigate the resolution bottleneck without sacrificing other performance metrics such as power consumption and refresh rate. Operation principles of the proposed technique are described in Section II. Sections III and IV address the multi-physics finite element analysis (FEA) and experimental measurements to further explore the performance metrics of the proposed technique.

II. Frequency Multiplexing for Resonance Selective Actuation in Vibrotactile Displays

Applying actuation force to suspended elements generate larger vibrations at the mechanical resonance frequency of these elements, i.e. taxels in this application. Supplying a single-tone sinusoidal current to an electromagnetic coil at frequency *f* generates proportional mechanical forces on soft ferromagnetic material at frequency *2f*. Hence, matching this frequency with the mechanical resonance frequency of a tactile element results in stronger vibrations in that element. We combine this principle with *frequency multiplexing*, originally used for increasing the bandwidth efficiency of telecommunication systems, to develop a new selective actuation technique. This new approach allows one single coil selectively control the vibrations of multiple taxels by supplying electrical currents at distinctive mechanical resonance frequencies of taxels. Hence, this technique can mitigate the resolution constraint in vibrotactile displays caused by using an individual coil for each taxel.

Figure 2a illustrates the 3D model of the proposed resonance-frequency selective actuation technique. Each taxel in the former prototype (See Figure 1) is replaced by two smaller taxels. These taxels have two different mechanical resonance frequencies (f_1 and f_2) in the new design. In this model two single-tone currents at frequencies $0.5f_1$ and $0.5f_2$ can be selectively supplied to the coil. Depending on the supplied current, this is expected to generate mechanical forces at frequencies f_1 and/or f_2 corresponding to the mechanical resonance frequencies of two taxels. Figure 2b shows the color-coded displacement of each taxel in response to the supplied electric current to the coil. The taxel on the right (or left) responds to the current supplied at frequency $0.5f_1$ (or $0.5f_2$).

For comparison with the first prototype shown in Figure 1, we developed a new 3D printed pad by replacing each taxel

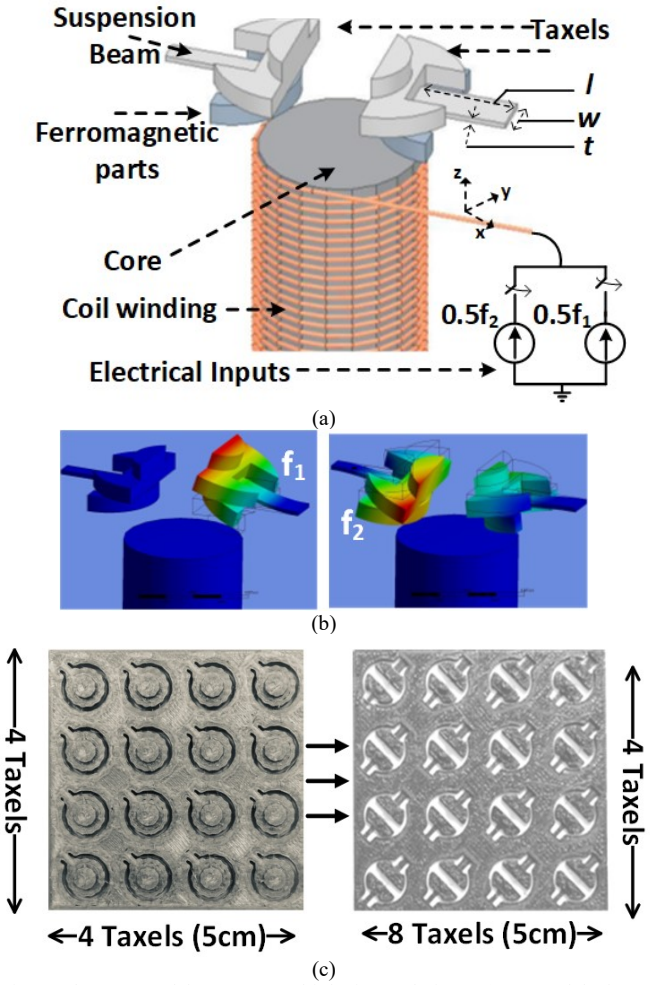

Fig. 2. The proposed frequency multiplexing technique, a) 3D model of two taxels on one coil supplied by two single-tone electrical currents, b) Magnetostatic Finite Element Analysis of two taxels with different resonance

with two half-taxels on the same area. The spatial resolution increase by two times in this prototype, i.e. from 16 to 32 taxels, is illustrated in Figure 2c, wherein both taxel arrays are printed using PLA material. Further increase in resolution can be achieved by dividing each taxel in the first prototype into three or more smaller taxels, which are all controlled by one actuator.

The taxel resonance behavior can be approximated by the general mass-spring model assuming that the mass is concentrated on the taxel and stiffness is only related to the suspension beam:

$$m\frac{d^2z}{dt^2} + \zeta\frac{dz}{dt} + kz = F \quad (1)$$

wherein z is the displacement of taxel in response to the applied force (F), and k, ζ and m represent the stiffness of suspension beam, the damping ratio and the taxel mass at the tip of the beam, respectively. Accordingly the resonance frequency of each taxel is determined by ω_n:

$$\omega_n = \sqrt{k/m} \quad (2)$$

The beam stiffness (k) is a function of its geometry. For the beams with rectangular cross section specifically, this is defined by the beam length (l), width (w) and thickness (t) as:

$$k \propto \frac{wt^3}{l^3} \qquad (3)$$

In this design the two half-taxels have identical tactile parts to make similar touch sensation whereas its individual resonance frequency can be tuned at different frequencies suitable for fingertip mechanoreceptors by changing the geometric parameters of suspension beams. We use the beam width only to tune the resonance frequencies of each taxel.

To further explore the operation of this new technique the electromagnetic force should be described in terms of the actuation input, i.e. the electrical current supplied to the solenoid coils. The perpendicular mechanical force applied to soft ferromagnetic material by a solenoid coil with *N*-turn winding that conduct electrical current *I* with cross-section area *A* at the far ends of coil, is described as follows [11]:

$$F = (\mu_0 \mu_r^2 \frac{N^2 A}{2l^2} \ln \mu_r) I^2 \qquad (4)$$

wherein μ_0, μ_r, and l are magnetic permeability of free space, relative permeability of solenoid iron core, and the solenoid length, respectively. Assuming that geometric and material coefficients are constant for each taxel, the mechanical force is proportional to the square of electrical current (I^2). Accordingly, suppling current at a certain frequency (f) to the solenoid generates a proportional mechanical force with doubled frequency ($2f$). Especially, supplying sinusoidal electrical currents ($i(t) = Isin(2\pi ft)$) at two different frequencies (f_1 and f_2) results in the following mechanical force applied to each taxel:

$$\begin{aligned} F &= \mu_0 \mu_r^2 \frac{N^2 A}{2l^2} \ln \mu_r \left(i_1(t) + i_2(t)\right)^2 \\ &= \mu_0 \mu_r^2 \frac{N^2 A}{2l^2} \ln \mu_r \left(I_1 sin(2\pi f_1 t) + I_2 sin(2\pi f_2 t)\right)^2 \\ &= \mu_0 \mu_r^2 \frac{N^2 A}{2l^2} \ln \mu_r \left(I_1^2 sin^2(2\pi f_1 t) \right. \\ &\qquad + 2 I_1 I_2 sin(2\pi f_1 t) sin(2\pi f_2 t) \\ &\qquad \left. + I_2^2 sin^2(2\pi f_2 t)\right)^2 \qquad (5) \end{aligned}$$

Hence, the solenoid converts the electrical power supplied at frequencies f_1 and f_2 to the mechanical force applied to each taxel at frequencies $2f_1$, $2f_2$, $f_1 \pm f_2$. Depending on the taxel resonance frequency, stronger vibrations are expected from each taxel in response to the excitation current at its corresponding frequency compared with any other excitation frequency. Hence, the selectivity of this approach depends on the magnitude of vibrations induced in each taxel in response to its corresponding excitation input. This will be further discussed in the following sections.

III. Multi-physics Finite Element Analysis (FEA)

Complicated modelling and verification of the real-world system using theoretical methods presented in Section II without idealistic assumptions suggest the application of multi-physics FEA tools. For example, the difference in material properties of the iron core and stainless steel washers underneath the taxels as well as the air gap between the taxels and coil are ignored in deriving the force function in Equations (4) and (5). Therefore, we developed a 3D multi-physics model using ANSYS Workbench to analyze the transient magnetic field generated by time varying electrical current at different frequencies and the mechanical force applied to the taxels. The displacement of taxels in response to applied electrical currents at different frequencies are also modeled using harmonic balance analysis.

The 3D model illustrated in Figure 2a, features a helix coil winding, which results in convergence issues for FEA solutions. At low frequencies though this helix can be replaced with a hollow cylinder as illustrated in Figure 3a. The top view

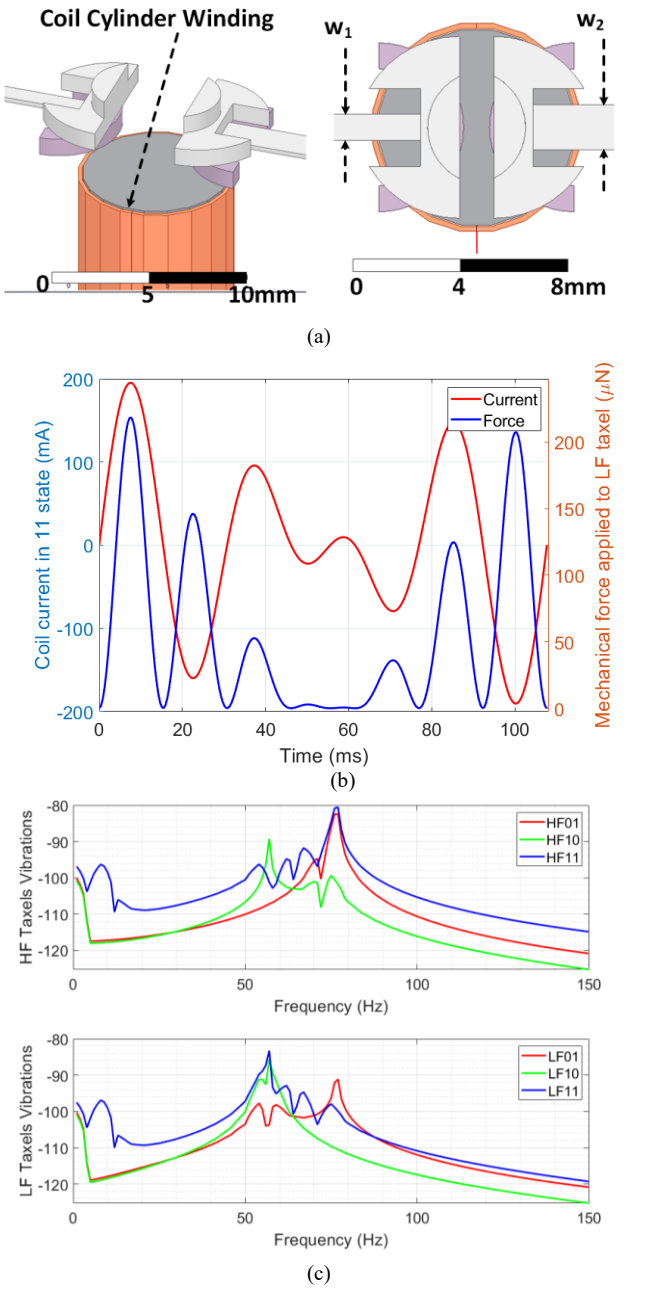

Fig. 3. Multi-physics FEA Model, a) the 3D model of actuator with cylinder winding: tilted side view (left) and top view (right), wherein the width of taxels w_1 and w_2 determines the difference in resonance frequencies, b) transient analysis of the force generated by actuator in response to the applied current at frequencies 28Hz and 38Hz, c) the frequency spectrum of taxel vibrations in response to three different coil excitation states: 01, 10, and 11.

TABLE I: DIGITAL STATES ASSOCIATED WITH ACTUATION INPUT AND CORRESPONDING VIBRATIONS

Digital input	Current supplied to the coil	Expected vibration
00	None	None
01	$I_2 sin(2\pi f_2 t)$	HF
10	$I_1 sin(2\pi f_1 t)$	LF
11	$I_1 sin(2\pi f_1 t) + I_2 sin(2\pi f_2 t)$	LF and HF

of this model shows the only asymmetry between the two taxels is in the width of their suspension beams to tune their resonance at slightly different frequencies (56 Hz for width w_1 and 74 Hz for width w_2). Two current inputs at two distinct frequencies (28 Hz and 37 Hz) are applied to the coil for both transient and magnetostatic analysis. The transient analysis results are shown in Figure 3b, wherein the coil converts the input current to mechanical force output. This energy conversion is associated with doubling the input electrical signal frequencies and adding additional spurious components at $f_1 \pm f_2$, as shown in Equation (5).

Harmonic Balance analysis are employed in this model to derive the vibration response of tactile elements to the input electrical signals in frequency domain. Tactile elements on vibrotactile displays are usually controlled by digital outputs from microprocessors. For example, in our initial prototype (See Figure 1), the supply of currents to coils are controlled by switching a power amplifier on/off via the microcontroller outputs. In order to analyze the proposed resonance-frequency selective actuation technique we associate digital states with actuator inputs and corresponding vibration outputs in Table 1. For example, digital state *01* describes the sinusoidal current with amplitude I_2 and frequency f_2, which should result in strong vibrations of taxel with resonance frequency $2f_2$, i.e. HF taxel. Assuming that $f_2 > f_1$, the high-frequency (HF) taxel responds with larger vibrations to excitation current at frequency f_2 whereas low-frequency (LF) taxel experiences larger vibrations in response to the excitation current at frequency f_1.

Two single-tone currents are applied individually (*01* and *10*) and together (*11*) following the terminology presented in Table 1 to run Harmonic Balance analysis on the meshed model of actuator. States *10* and *01* correspond to single-tone current inputs at 28Hz and 38Hz, respectively, whereas state *11* input consists of two single-tone input added together. The simulation results are illustrated in Figure 3c. HF and LF taxels respond with stronger vibrations to inputs *01* and *10* with peak vibrations at around 56Hz and 76Hz, respectively. In addition, HF and LF vibrations are more than 10dB weaker to the opposite excitation, which shows a good isolation, i.e. selectivity, between the two taxels. Input *11* results in stronger vibrations at resonance frequencies of LF and HF while generating two additional spurious components at $f_1 \pm f_2$.

IV. CHARACTERIZATION AND DISCUSSION

The 3D printed taxel pair and the measurement setup are illustrated in Figure 4. For characterization purposes we printed two PLA taxels anchored to a rectangular substrate as shown in Figures 4a and b. The resonance frequency of these two taxels are adjusted by the width of suspension beams only for the sake

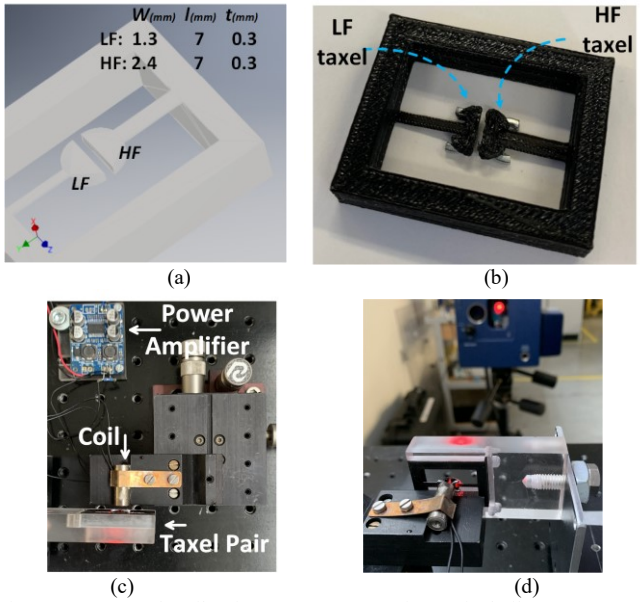

Fig. 4. Test setup for vibration measurement using optical vibrometry, a) 3D model for the taxel pair, b) 3D printed taxel pair in PLA, c) top view of the test setup: power amplifier module, 3D printed taxels, and solenoid coil fixed to a micromanipulator, d) test setup in front of PSV-500 optical vibrometer.

of simplicity. Other aspects such as length and thickness of these beams add flexibility in the design of taxels with different resonance frequencies on a small area. The dimensions of suspension beams are reported on the 3D model in Figure 4a. Two stainless steel washers are glued to the back side of printed taxels as shown in Figure 4b. The taxel pair is fixed on a stand opposite to the coil that is mounted on a micromanipulator on a vibration isolation table as illustrated in Figure 4c, wherein the coil current is supplied through a power amplifier module. The micromanipulator allows the position of coil to be adjusted with respect to the taxels.

For vibration measurements we use high-precision optical vibrometer (PSV500), which receives the reflection of a laser beam from each taxel. The whole setup is fixed on a vibration isolation table in front of the optical vibrometer as demonstrated

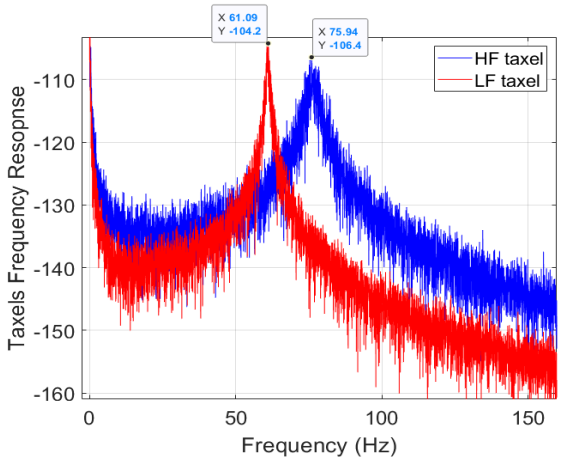

Fig. 5. Optical characterization of the taxel pair resonance behavior: displacement measurement of taxel vibrations

in Figure 4d. Initially we used this setup to extract the resonance

behavior of taxels. Electrical white noise is supplied form PSV inbuilt signal generator to the coil through the power amplifier module while the laser measures the vibration amplitude. The displacement measurement results are shown in Figure 5. The resonance frequency of printed LF and HF taxels are at around 61Hz and 76Hz, respectively. The difference between resonance frequencies for the designed taxel model (56Hz, 76Hz) and real-world samples (61Hz and 76Hz) might be due to the printing precision of the 3D printer and/or the stress applied to the LF sample while removing from the printer plate. It should be noted that this measurement is repeated for each taxel by shifting the coordinates of laser spot from HF to LF taxels. The resonance amplitude of the HF taxel is around 2dB lower, which might be related to the higher stiffness of its wider suspension beam that was designed to increase its resonance frequency. The quality factor (Q) of taxel resonators determine the selectivity performance of this technique, i.e. the higher Q-factor allows taxels to be designed at closer resonance

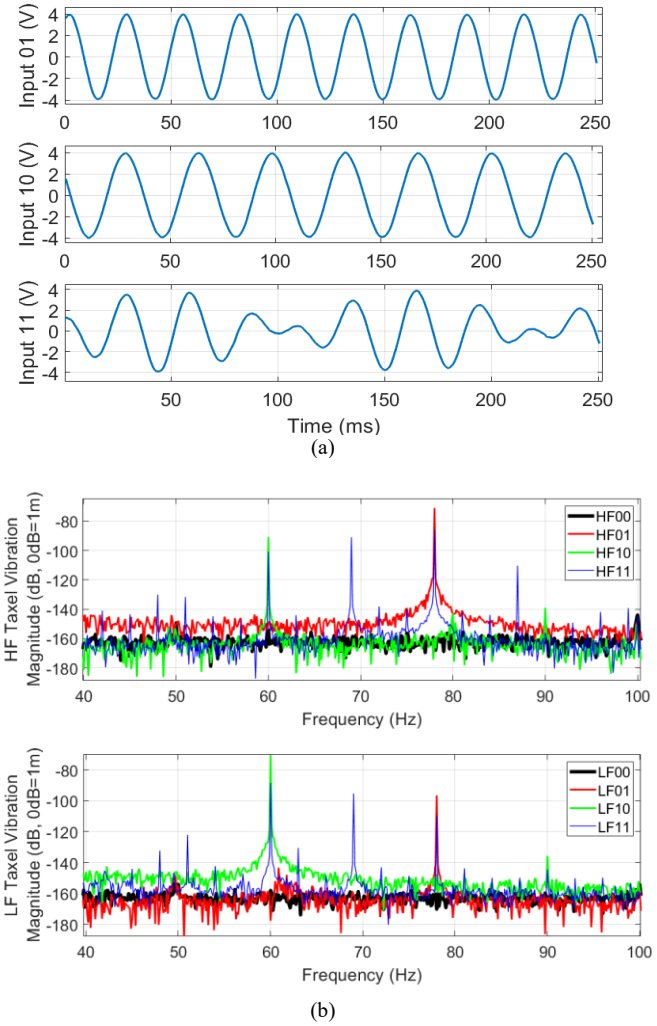

Fig. 6. Optical vibration measurement for the taxels, a) The measured actuation input voltages supplied to the coil in three actuation states 01 (38Hz) 10 (30Hz), and 11 (30Hz + 38Hz), b) Optical characterization of the resonance-selective actuation behavior for LF (bottom) and HF (top) taxels in frequency domain.

frequencies. As illustrated in Figure 5, with these taxels maximum mechanical decoupling between two neighboring taxels is around 15dB. This has been further discussed after measuring the vibration response of taxels to individual inputs.

Vibration response of taxels are measured while applying the corresponding input states. Time domain voltage signals applied to the coil are shown in Figure 6a for three different states. Inputs *01*, *10* and *11* represent sinusoidal voltages at 30Hz, 38Hz and 30Hz+38Hz, respectively, which drives proportional currents in the coil. The coil resistance (62.9Ω) and inductance (41.7mH) are measured using an LCR meter at frequencies below 100Hz, wherein the coil reactance is negligible compared with its resistance. Hence the corresponding coil current may be derived from dividing the voltage by resistance value. The resistance and inductance vary from 62Ω to 65Ω and from 41.9mH to 40.8mH, over this frequency range.

The frequency spectrum of each taxel displacement output is individually measured using the optical vibrometer setup in Figure 4. Accordingly, each taxel is actuated by applying the inputs illustrated in Figure 6a. The PSV displacement output is recorded for HF and LF taxel vibrations separately. The results are presented for different actuation states in Figure 6b (Hf taxel at the top and LF taxel at the bottom). These measurements run over 2~200Hz bandwidth with 3200 FFT points. The automatic laser beam focus was repeated for each taxel by PSV controller to achieve maximum signal-to-noise ratio. The resonance peaks of each taxel are visible at around 60Hz and 78Hz in response to 30Hz (state *10*) and 38Hz (state *01*) actuation inputs, respectively. The *01* state must ideally actuate HF taxel only, however, due to limited Q factor it actuates LF taxel too but at around 25 dB lower vibration magnitude (See red spectrums in Figure 7b bottom). Similarly, in response to *10* state, HF taxel shows 20 dB smaller vibrations (See the green spectrums in Figure 7b top). This selectivity of the proposed actuator in creating distinctive mechanical impacts for different states is a function of the Q-factor of taxels. Consequently, the maximum number of taxels that can be selectively actuated by one coil, i.e. the upper limit for resolution increase, is determined by the taxel Q-factor.

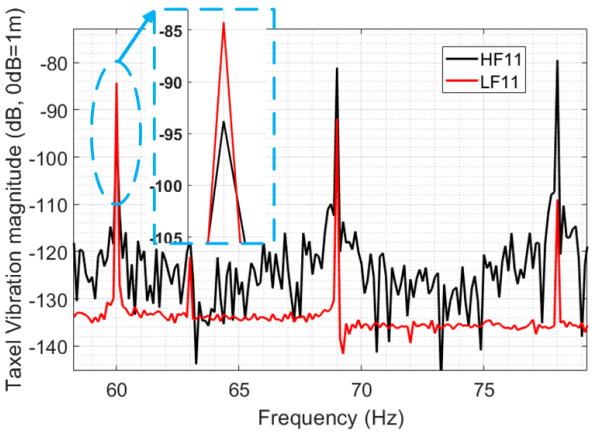

Figure 7: State *11* vibrations measured on LF and HF taxels after increasing the input power.

The actuator response to state *11*, however is around 10dB

smaller than two other states for both taxels as shown in Figure 6b. This is caused by spreading the power of two electrical current sources ($f_1 \pm f_2$) over four frequencies ($2f_1$, $2f_2$ *and* $f_1 \pm f_2$) compared to previous states, wherein the power of each electric current source is concentrated at one single frequency. Hence, for state *11* we increased the power level on both frequencies to reach the vibration level shown by two other single-tone states. This calibration result is shown in Figure 7, wherein the taxel responses to state *11* with larger input voltage (around 5Vp) are measured in the same vibrometry setup. Further increase results in higher power consumption which is being wasted at spur frequency components. This could be alleviated by means of additional signal processing just before applying the voltage signal to power amplifier to remove the spur frequency components.

In this prototype, the response of taxels to excitation frequencies are precisely reproducible. This has been successfully tested by applying excitations frequencies to five different replicas of taxel pairs implemented by bench-top 3D printers. However, for smaller taxels, the displacement measurement might be needed to detect the resonance frequency and adjust the excitation frequency accordingly, which reduces the resonance sensitivity to manufacturing inaccuracies.

The resolution improvement achieved by this new technique depends on the number of taxels that can be vibrated by one actuator, i.e., the number of resonances that fit within the frequency range perceivable by the sense of touch. Here, we derive the maximum spatial resolution as a function of the quality factor of each taxel (Q_i), which is defined as the ratio of resonance frequency (f_i) divided by the *3dB* bandwidth (Δf_{3dB}),

$$Q_i \equiv \frac{f_i}{\Delta f_{3dB}} \quad (6)$$

Adjacent taxels require a minimum difference in the vibration amplitudes perceived as ON/OFF states. This threshold for the vibration ratio is represented by Δy in Figure 8. Hence, the

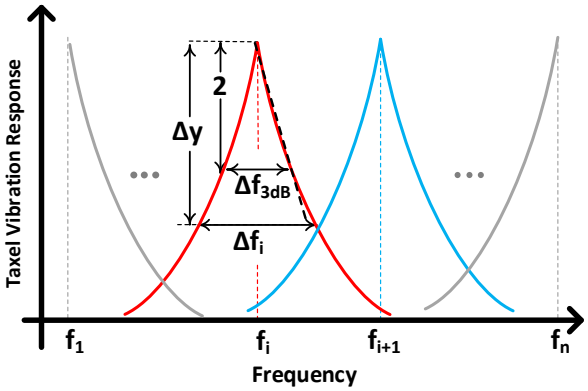

Figure 8: The frequency response of multiple taxels with different resonance frequencies.

minimum bandwidth required for ith taxel (Δf_i) to avoid interference between adjacent i^{th} and $(i+1)^{th}$ taxels can be obtained by the linear approximation represented by the dashed lines in Figure 8:

$$\frac{\Delta f_{3dBi}}{2} \cong \frac{\Delta f_i}{\Delta y} \quad (7)$$

In order to increase the resolution by exploiting the full available bandwidth for n taxels without interference, Δf_i must satisfy the following equation, which is obtained by replacing (6) in (7):

$$\Delta f_i \cong \frac{\Delta y f_i}{2Q_i} \quad (8)$$

From Figure 8, the distance between two consequent resonance frequencies is described as:

$$f_{i+1} - f_i = \frac{\Delta f_i}{2} + \frac{\Delta f_{i+1}}{2} \quad (9)$$

Assuming that Q is the minimum quality factor of the taxels and replacing (8) in (9),

$$\frac{f_{i+1}}{f_i} = \frac{1 + \frac{\Delta y}{4Q}}{1 - \frac{\Delta y}{4Q}} \quad (10)$$

whereby the maximum number of taxels can be obtained from the ratio of the highest resonance frequency (f_n) to the first resonance frequency (f_1):

$$\frac{f_n}{f_1} = \left(\frac{1 + \frac{\Delta y}{4Q}}{1 - \frac{\Delta y}{4Q}}\right)^n \quad (11)$$

$$n = \frac{\log\left(\frac{f_n}{f_1}\right)}{\log\left(\frac{1 + \frac{\Delta y}{4Q}}{1 - \frac{\Delta y}{4Q}}\right)} \quad (12)$$

The perceivable vibrotactile frequencies roughly range between 20Hz-1000Hz, which reaches to its maximum at 250Hz [12]. The minimum Q for the 3D printed taxels in this work is around 15. Assuming the vibration threshold for adjacent taxels is Δy=10, from equation (12) the maximum number of taxels controlled by one coil is $n = 11$ in this prototype.

V. Conclusion

The limited spatial resolution of vibrotactile displays has hindered its real-world applications. This limit is mainly caused by the actuator size that vibrate individual tactile elements in a vibrotactile display. We presented a new resonance-frequency selective electromagnetic actuation technique to alleviate the resolution bottleneck. The proposed method for increasing the resolution whereby one coil controls multiple taxels makes the total resolution independent of the size of the coil and the pitch spacing between the coils. This new technique has been implemented in a low-cost and highly reliable process by means of 3D printed tactile pad and off-the-shelf components. Although replacing each taxel by two halfz -taxels resulted in two times resolution increase in this prototype, further increase in the resolution is only limited by the Q-factor of taxels that determines the selectivity of actuator i.e. how close the resonance frequencies can be selected in the design process. Multi-physics finite element analysis and optical vibrometry experiments demonstrate a strong agreement between the design hypothesis, simulation results and experimental

measurements. The proposed actuation technique have significant potential to increase the information that can be conveyed via vibrotactile displays without sacrificing other performance metrics such as power consumption and refresh rates.

REFERENCES

[1] M. Hafez, "Tactile interfaces: technologies, applications and challenges," *Vis. Comput.,* vol. 23, no. 4, pp. 267-272, 2007.

[2] M. Tezuka, N. Kitamura, K. Tanaka, and N. Miki, "Presentation of various tactile sensations using micro-needle electrotactile display," *PloS one,* vol. 11, no. 2, p. e0148410, 2016.

[3] Q. Wang and V. Hayward, "Biomechanically optimized distributed tactile transducer based on lateral skin deformation," *Int. J. Robotics Res.,* vol. 29, no. 4, pp. 323-335, 2010.

[4] X. Xie, Y. Zaitsev, L. F. Velásquez-García, S. J. Teller, and C. Livermore, "Scalable, MEMS-enabled, vibrational tactile actuators for high resolution tactile displays," *Jnl. of Micromech. and Microeng.,* vol. 24, no. 12, p. 125014, 2014.

[5] J. J. Zárate and H. Shea, "Using pot-magnets to enable stable and scalable electromagnetic tactile displays," *IEEE Trans. Haptics,* vol. 10, no. 1, pp. 106-112, 2016.

[6] J. Streque, A. Talbi, P. Pernod, and V. Preobrazhensky, "New magnetic microactuator design based on PDMS elastomer and MEMS technologies for tactile display," *IEEE Trans. Haptics,* vol. 3, no. 2, pp. 88-97, 2010.

[7] M. Benali-Khoudja, M. Hafez, J.-M. Alexandre, and A. Kheddar, "Electromagnetically driven high-density tactile interface based on a multi-layer approach," in *IEEE Symposium on Micromechatronics and Human Science*, 2003, pp. 147-152.

[8] H. Ishizuka and N. Miki, "MEMS-based tactile displays," *Displays,* vol. 37, pp. 25-32, 2015.

[9] H. Ishizuka, K. Suzuki, K. Terao, H. Takao, F. Shimokawa, and H. Kajimoto, "Development of a multi-electrode electrovibration tactile display with 1 mm resolution," in *IEEE World Haptics Conference*, 2017, pp. 659-664.

[10] A. Mohammadi, N. Karmakar, and M. Yuce, "A post-fabrication selective magnetic annealing technique in standard MEMS processes," *Appl. Phys. Lett.,* vol. 109, no. 22, p. 221906, 2016.

[11] P. H. Schimpf, "A detailed explanation of solenoid force," *Int. J. Recent Trends Eng.Technol. (IJRTET),* vol. 8, no. 2, p. 7, 2013.

[12] E. L. Gunther, "Skinscape: A tool for composition in the tactile modality," Massachusetts Institute of Technology, 2001.